Meso-2-MethoxyNaphthalenyl-BODIPY as Efficient Organic Dye for Metallaphotoredox Catalysis

Meso-2-MethoxyNaphthalenyl-BODIPY as Efficient Organic Dye for Metallaphotoredox catalysis

Elena Bassan,[a][b] Francesco Calogero,[a][b] Yasi Dai,[a] Angela Dellai,[a] Alessandro Franceschinis,[a] Emanuele Pinosa,[a][b] Fabrizia Negri,[a] Andrea Gualandi,*[a][b] Paola Ceroni,*[a][b] Pier Giorgio Cozzi*[a],[b]

[a] Dipartimento di Chimica "Giacomo Ciamician"
Alma Mater Studiorum – Università di Bologna
Via Selmi 2, 40126 Bologna, Italy
E-mail: andrea.gualandi10@unibo.it; paola.ceroni@unibo.it; piergiorgio.cozzi@unibo.it

[b] Center for Chemical Catalysis – C3
Alma Mater Studiorum – Università di Bologna
Via Selmi 2, 40126 Bologna, Italy

Supporting information for this article is given via a link at the end of the document.

Abstract: A new *meso*–naphthalenyl BODIPY was designed for the efficient generation of long-lived triplet excited state under irradiation with green light. The new, heavy atom-free organic chromophore was employed in a benchmark example of dual palladium and photoredox catalysis, highlighting the applications of BODIPY dyes as photoredox catalysts.

Introduction

The synthetic chemistry community has been deeply influenced, in the last decade, by a growing interest in the field of visible–light mediated photocatalysis. In fact, for a long time, most of the examples in which light radiation was employed to promote synthetic organic transformations were related to the use of high energy UV light. However, the hazards associated with such short wavelengths, together with the lack of selectivity of the reported processes hampered the possible developments of light-mediated protocols and their widespread applicability. As soon as organometallic complexes and organic dyes were realized to have interesting photophysical properties coupled to visible light absorption, photochemistry was subjected to renaissance. Among a plethora of photochemical reactions, the most commonly employed photoreactions in organic synthesis are photoinduced electron transfer processes between the photoexcited dye and an organic substrate, allowing the generation of radical species[1] in unprecedentedly mild reaction conditions.[2]

The widespread acceptance and the development of this field was possible due to the well-established photophysical properties of the photoredox catalysts.

The first examples of photoredox catalysis, using low energy visible light, employed the well-known polypyridyl complexes of ruthenium or iridium. One of the advantages of these metal complexes is their highly efficient (100% in most of the cases) population of the lowest triplet excited state, related to the presence of heavy metal ions. This triplet excited state is characterized by a sufficiently long lifetime (of the order of 1-10 μs) to be involved in efficient photoinduced electron transfer processes with organic substrates.

Additionally, these photocatalysts can be merged with transition metal co-catalysts[3] in dual synergistic catalysis.[4] In fact, a key methodology for the modification of a metal's oxidation state traditionally consists in the addition of stoichiometric oxidants or reductants, which enables–the formation of C–C or C–X (X= O, N, S) bonds.[4] The same change of oxidation state can be performed by photoinduced electron transfer with properly designed photocatalysts, allowing bond formation and breakage under mild reaction conditions.[5] However, the scarcity of ruthenium and iridium, their high costs, and the tedious synthesis of the complexes, accompanied by generation of heavy metal waste, have stimulated chemists towards the exploration of new photocatalysts,[6] such as metal-free organic chromophores.[7] Unfortunately, most of the reported organic dyes do not efficiently populate their long-lived triplet excited states.

Boron dipyrromethene (BODIPY) derivatives[8] are traditionally known as brightly fluorescent dyes, which couple a high fluorescence quantum yield with a high molar absorption coefficient in the visible spectral region, as well as a high photostability. Recently, a huge interest has emerged for BODIPY dyes that exhibit efficient population of their long-lived triplet state (T_1).[8,9] For this class of dyes, a strong reduction of fluorescence quantum yields is accompanied by the emergence of phosphorescence and/or sensitization of singlet oxygen by energy transfer from T_1 state. The most extensively utilized strategy to promote the population of T_1 has been the insertion of iodine or bromine atoms on the pyrrolic units, which strongly increases spin-orbit coupling (SOC) by the heavy atom effect and thus favors the population of the triplet state.[10] This has therefore extended the fields in which BODIPYs find applications to those of photodynamic therapy[11] and photocatalysis.[12] However, halogenation of the BODIPY core inevitably shifts the reduction potential to less negative values, consequently limiting their employment in photoredox transformations.[13]

A different approach relies on dyads in which the BODIPY core is covalently linked in the *meso* position to an orthogonally-oriented electron donating moiety, such as in our case 2-methoxynaphthalene (Figure 1). The design is such that, upon excitation of the BODIPY core (green arrow in Figure 2), a photoinduced electron transfer (PeT) from the donor unit to the boron dipyrromethene unit takes place, leading to the population of a charge-transfer singlet excited state (^{1}CT, Figure 2). This decays by charge recombination to form the T_1 state localized on the BODIPY unit,[8,14] which can react with a substrate or generate singlet oxygen, thanks to its long-lived excited state.[15]

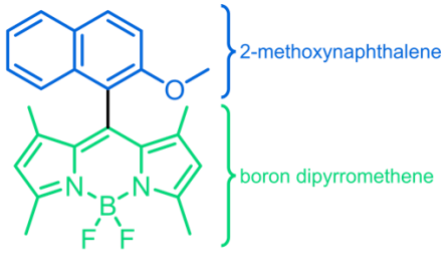

Figure 1. BODIPY dyad, BDP, **1** employed in this work.

Noteworthily, this strategy allows to independently tune the population of the triplet state and the values of its redox potentials. Indeed, functionalization of boron dipyrromethene's *meso* position does not strongly influence the energy of its HOMO (H) and LUMO (L) orbitals.[16] By this approach, both T_1 excited state and ground state potentials can be engineered to be strong reductants or oxidants, an important property for photocatalytic applications. Lastly, it is worth highlighting that introduction of alkyl groups in 2,4 positions of the pyrrolic rings are needed to secure the orthogonal orientation of the dyad's constituting units and, at the same time, protect the boron dipyrromethene core from radical attack or polymerizations.[17]

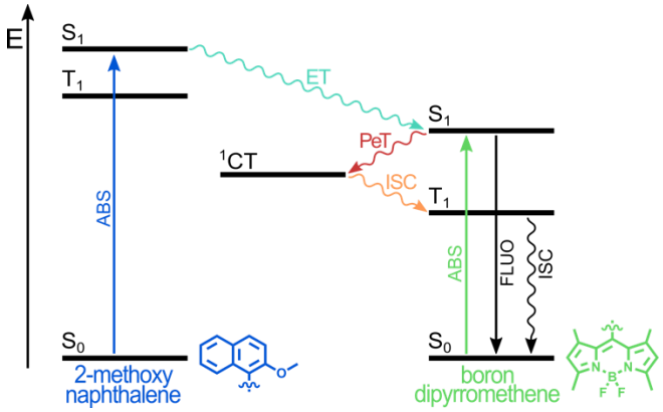

Figure 2. Jablonski diagram illustrating the main steps in the formation of the triplet state in the case of **BDP**. ET= energy transfer; PeT= photoinduced electron transfer; ISC= intersystem crossing; ABS= absorption; FLUO= fluorescence.

Based on these premises, we investigated the possible role of **BDP** dyad (Figure 1), which features an electron donating 2-methoxynaphtyl unit orthogonally placed compared to the BODIPY plane, as photosensitizer to carry out a C–C bond formation reaction in the presence of a palladium catalyst. Up until now, this has been an almost unexplored field for BODIPY dyes, with only a few examples reporting the use of iodinated BODIPYs in Atom Transfer Radical Addition (ATRA) reactions[18] or oxidations mediated by $O_2^{\bullet-}$[19] and only one example of a fluorescent BODIPY dye used in metallaphotoredox catalysis.[10] To the best of our knowledge, this is the first example in which a BODIPY dyad is used as a photocatalyst in photoredox catalysis and, more specifically, in which a triplet-populating BODIPY is used in metallaphotoredox catalysis.

Results and Discussion

BDP was prepared in good yields by a slight modification of usual protocols employed for the *meso*-BODIPY synthesis (see SI for details). The molar absorption coefficient of **BDP** is very high in the visible region: 91700 $M^{-1}cm^{-1}$ at 502 nm in MeCN (Figure 3A and Table 1), much higher than that of the prototypical $[Ru(bpy)_3]^{2+}$ dye (13000 $M^{-1}cm^{-1}$ at 452 nm in MeCN.[21] In addition, the absorption spectrum of the dyad shows the contribution of the naphthalene chromophore in the range of 250-350 nm, with absorption bands slightly shifted compared to the model compound 2-methoxynaphthalene. Therefore, the electronic interaction between the two chromophoric units of the dyad is limited, in accordance with the orthogonal geometry between the electron donating unit and the BODIPY core (Figure 1). Indeed, the ^{19}F spectra recorded for the **BDP** show two distinct sets of resonances, as the spectra display inequivalence of the heterotopic fluorine atoms, as each fluorine atom residing in two distinctly different environments.[22] In fact, instead of observing a standard quartet, we recorded a ^{19}F spectrum with two distinct doublet of quartets (see SI) due to the $^1J(^{19}F\text{-}^{11}B)$ and the strong $^2J(^{19}F\text{-}^{19}F)$ with satellite peaks from additional coupling to ^{10}B.
Although 2-methoxynaphthalene is fluorescent (λ_{FLUO}^{MAX}= 350nm, Figure 3B), excitation of the naphthyl group in the dyad only yields emission from the BODIPY core and the excitation spectrum performed at the emission maximum of the BODIPY core matches the

absorption spectrum of the dyad. This result indicates that energy transfer between these two units takes place with unitary efficiency (Figure 2, 3B and Figure S4). The quantum yield for **BDP**'s fluorescence has been measured as 60%; the quantum yield for the sensitization of singlet oxygen ($^1O_2$) is 27%, which means that the dyad is able to populate its long-lived triplet excited state (T_1).[23] Since no phosphorescence was detected in either degassed solutions or at 77 K, the lifetime of T_1 was determined by transient absorption spectroscopy and is equal to 48 μs (Figure S6). Additionally, electrochemical characterization (Figure S7) revealed that both oxidation (+1.15 V vs SCE) and reduction (-1.15 V vs SCE) processes are chemically reversible, which is beneficial for the employment of **BDP** as photocatalyst in catalytic cycles. These redox potentials are comparable with those previously reported for the sole BODIPY core[24] and further confirm the fact that the two units are electronically decoupled.

To assist the analysis of photophysical data we carried out a computational investigation on **BDP**. Notably, the optimized ground state geometry of the donor (2-methoxynaphthalenyl) and the acceptor unit of **BDP** demonstrates that they are arranged in an orthogonal orientation with the dihedral angle connecting the subunits of the dyad close to 90° and the two subunits essentially decoupled (Figure S12). Inclusion of solvent effects shows a stabilization of the ground state owing to the significant dipole moment of the dyad (Table S2). The effect of the solvent on the structural parameters is however modest, as shown in Figure S12**.** Because of the orthogonal structure, molecular orbitals (MOs) can be distinguished into a set of donor-localized and a set of acceptor-localized orbitals (Figure 4 and S13). We note that the H/L energies of **BDP** are not very different from those of boron dipyrromethene (Figure 1, Table S3) which agrees with the modest changes in redox potentials determined for **BDP**.

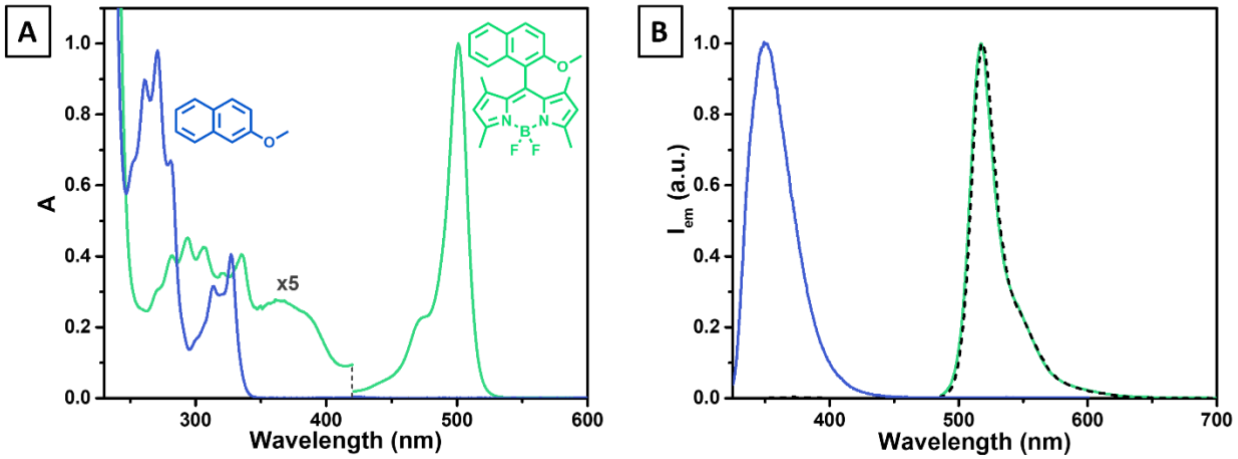

Figure 3. A) Normalized absorption spectra of **BDP** (green) and 2-methoxynaphthalene (blue) in MeCN. B) Normalized fluorescence spectra in MeCN of **BDP** with λ_{exc}= 480nm (green); **BDP** with λ_{exc}= 280nm (dashed line) and 2-methoxynaphthalene (blue, λ_{exc}= 310nm).

Table 1. Photophysical and electrochemical characterization of **BDP** in MeCN. [a]Degassed MeOH solution. [b]V vs SCE, in MeCN/$TEAPF_6$ 0.1M.

	ε ($M^{-1}cm^{-1}$)	λ_{MAX}^{ABS} (nm)	λ_{MAX}^{FLUO} (nm)	ϕ_{FLUO}	τ_{S_1} (ns)	ϕ_Δ	τ_{T_1} (μs)[a]	E(**BDP**$^{\bullet+}$/**BDP**)[b]	E(**BDP**/**BDP**$^{\bullet-}$)[b]
BDP	91700	501	518	60%	5.9	27%	48	+1.15	-1.15

The time-dependent (TD)-DFT calculations at the ground state geometry reveal the nature of the low-lying excited states of **BDP** and the role of solvent effect. To analyze in more detail the experimental absorption bands we calculated vertical excitations also for high lying singlet excited states to assign not only the strongest band in the spectrum but also the additional weaker features (Table S4). Because the donor and acceptor units of the dyad are orthogonal in the ground state, electronic transitions are essentially localized on one or the other unit. The observed bands are indeed readily assigned to computed local excitations (Table S4) as shown in Figure S15. In addition, charge transfer (CT) excitations are identified from the calculations, although it is not possible to assign them to experimental bands owing to their negligible oscillator strength.

TD-DFT calculations show that the lowest energy ^{1}CT state is dominated by the $H-1 \rightarrow L$ excitation which implies a CT from the 2-methoxynaphthalene unit to the BODIPY core (Figure 4) with an excited state dipole moment remarkably increased compared to the ground state (Table S2). Solvent stabilization on ^{1}CT state is crucial for the photoinduced processes occurring on **BDP**. To get some insight on its magnitude, we carried out state specific (SS) corrected linear response (cLR) TD-DFT calculations at the ground state geometry in MeCN both with the fast solvent component equilibrated (NEQ) and with fully equilibrated solvent (EQ) on the excited states. The results at the ground state geometry (Figure S17) show a remarkable stabilization of the ^{1}CT state outlining the relevant role of this state in the investigated dyad. Unfortunately, we could not determine the equilibrium structure of the ^{1}CT state due to

technical issues, namely the impossibility of using the cLR approach for the excited state optimization and the overstabilization of the S_1 state which prevented the optimization of ^{1}CT with the LR approach.

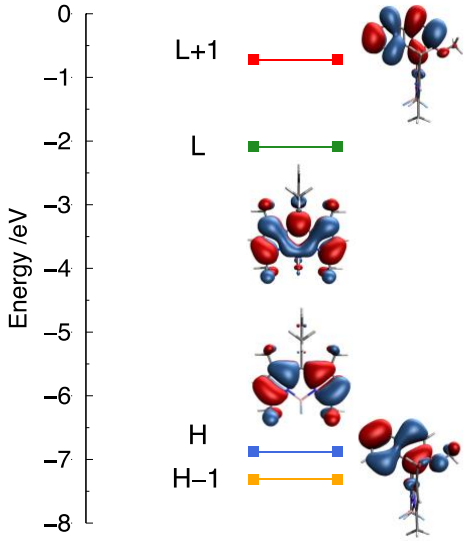

Figure 4. Energies and shapes of the frontier molecular orbitals of **BDP**. MeCN-M06-2X/6-311G* calculations.

Nevertheless, we were able to obtain the equilibrium geometry of the ^{3}CT state which shares a similar wavefunction with ^{1}CT (Table S4). This geometry (Figure S18) can be assumed as representative of the ^{1}CT equilibrium structure. Hereafter, it will be labelled as CT and will be considered for the spin-orbit coupling (SOC) calculations. Notably, such CT geometry is twisted with a twisting angle between the donor and acceptor subunits of around 123°.

The intersystem crossing (ISC) process can be discussed in terms of a simplified relation (*Equation 1*), where the rate constant (k_{ISC}) is proportional to the square of the SOC matrix element $\langle T_n|\widehat{H_{SO}}|S_n\rangle$:[25,26]

$$k_{ISC} \propto \left|\langle T_n|\widehat{H_{SO}}|S_n\rangle\right|^2 \qquad (1)$$

Therefore, to assess the efficiency of the ^{1}CT→T_1 ISC process we determined SOC interactions both at ground state and CT equilibrium geometries. Table 2 shows a $\langle T_1|\widehat{H_{SO}}|\,^1CT\rangle$ value twice as big at the CT geometry compared to the one calculated at the ground state geometry, implying an efficient population of the T_1 state via ISC for **BDP**. These results are in good agreement with photophysical measurements and support the photocatalytic efficiency of **BDP** via triplet state population.

Table 2. Computed SOC magnitudes between ^{1}CT and T_1 states of BDP at the ground state and CT geometries.

Geometry	SOC ^{1}CT/T_1 (cm^{-1})[a]
Ground state	0.64
CT	1.35

[a] SOC values calculated with the SOMF(1X) approach including relativistic corrections with ZORA, from TDA-M06-2X/ZORA-def2-TZVP calculations.

We have recently applied a diiodo-BODIPY dye for the C– C bond formation via ATRA, in combination with sodium ascorbate.[18] The reaction was extremely sensitive to trace of oxygen, and we were unable to extend these findings in metallaphotoredox catalysis.[18a] To the best of our knowledge, the ability of triplet BODIPY to induce photoredox transformations in the presence of metals was not demonstrated yet. To study the possibility of using BODIPY in metal promoted transformations we selected the reaction described by Sanford in 2011, which can be considered as the first application of photoredox catalysis in combination with transition metal catalysis.[27] The reaction developed by Sanford was a Pd(II)/Pd(IV)[28] C–H arylation with diazonium salt,[29] in the presence of $[Ru(bpy)_3Cl_2]$ as photocatalyst. The reaction was further developed to include different heterocycles and directing groups.[30] In addition, organic photoreductants were able to promote the reaction. (*N*-Et)AcrH_2 (9,10-dihydro-10-ethylacridine) was reported as an active organic photocatalyst in the dual catalytic direct C–H arylation of various substituted acetanilides and benzamides under blue LEDs irradiation (λ_{max} = 425 nm).[31] Additionally, a dual Pd direct C-H arylation of electron-rich anilides promoted by eosin-Y was also reported using, this time, green light.[32] The photocatalyst reduces the diazonium salt forming an aryl radical that was intercepted by a palladacycle-Pd(II) complex (generated by C–H activation of the substrate) giving a Pd(III)Aryl intermediate. Oxidation by the photocatalyst of the intermediate Pd(III) to Pd(IV) complex favors the reductive elimination for the formation of the final product and regenerates the Pd(II) complex and the photocatalyst in its original form.[28b] This reaction was also reported with the employment of organic dyes as photocatalysts[29] and can be considered a benchmark reaction to test new photocatalysts for metallaphotoredox reaction promoted by palladium.

We commenced our investigation by exploring the best reaction condition for the transformation of 2-(*o*-tolyl)pyridine **2a** as the model substrate (Table 3).

Table 3. Optimization of the reaction parameters.

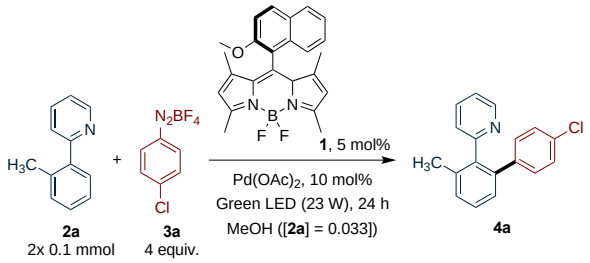

2a 2x 0.1 mmol | **3a** 4 equiv. | **4a**

Entry[a]	Deviation from standard conditions	Conversion %[b]
1	None	>99(72)
2	No light	16(12)[c]
3	No **1**	16
4	No $Pd(OAc)_2$	NR
5	**1,** 2.5 mol%	85
6	**1**, 1 mol%	21
7	**1,** 2.5 mol% and [**2a**] = 0.1 M	53
8	**1,** 2.5 mol% and $Pd(OAc)_2$ 5 mol%	85
9	**3a**, 2 equivalents	50
10	Kessil Green LED (40W)	>99
11	60 h irradiation time	>99[d]
12	DMF instead of MeOH	17
13	DMSO instead of MeOH	48
14	CH_3CN instead of MeOH	0
15	$Pd(PPh_3)_4$ instead of $Pd(OAc)_2$	0
16	$PdCl_2(PPh_3)_2$ instead of $Pd(OAc)_2$	0

[a] Reaction performed in double on 0.1 mmol at room temperature. [b] Conversion determined by ^1H NMR. Isolated yields after chromatographic purification in parenthesis. [c] The reaction was also conducted at 35 °C and a conversion of 23% was observed. [d] The reaction shows the presence of unidentified byproducts, in crude ^1H NMR, although the conversion was complete. NR = no reaction.

Small amount of product was observed in the reaction performed in absence of light or **1** (Table 3, entries 2 and 3 respectively), as was also reported by Sandford, due to the presence of the palladium complexes and formation of aryl radical.[27] Irradiation with green light resulted sufficient to promote the reaction and a yield comparable with the previous work was obtained (Table 3, entry 10). Also, in our case it turned out that the optimal solvent was MeOH while other solvents were found not suitable for the reaction (Table 3, entries 12-14). Different palladium sources were found to be inactive in the reaction (Table 3, entries 15 and 16). The reaction was investigated using a powerful light source (entry 10) and no by-product was revealed. Instead, unidentified by-products were formed prolonging the reaction time.

With the optimized reaction conditions in our hand, we explored the scope of the reaction, by varying first the diazonium compounds (Scheme 1) and extending the reaction time to 48 hours to have consistent results between differently reactive substrates. Substituted electron rich and poor diazonium derivatives, simply prepared by standard conditions (see SI for details), reacted in moderate to good yields with **2a** affording the desired compounds **4b-e**. In the case of **3e**, we have also isolated **4c** in 11% yield due to a successive S_NAr reaction of solvent (MeOH) with **3c** (Scheme 1).

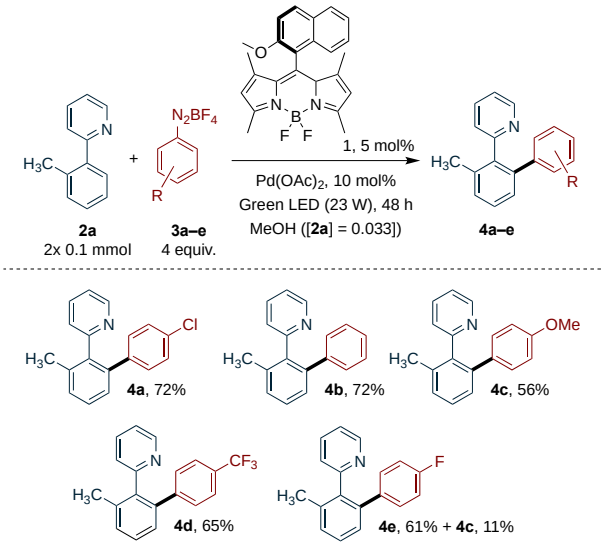

Scheme 1. Survey of different aryl diazonium salt.

Then, we tested differently substituted pyridines and other scaffolds, and the results collected are depicted in Scheme 2.

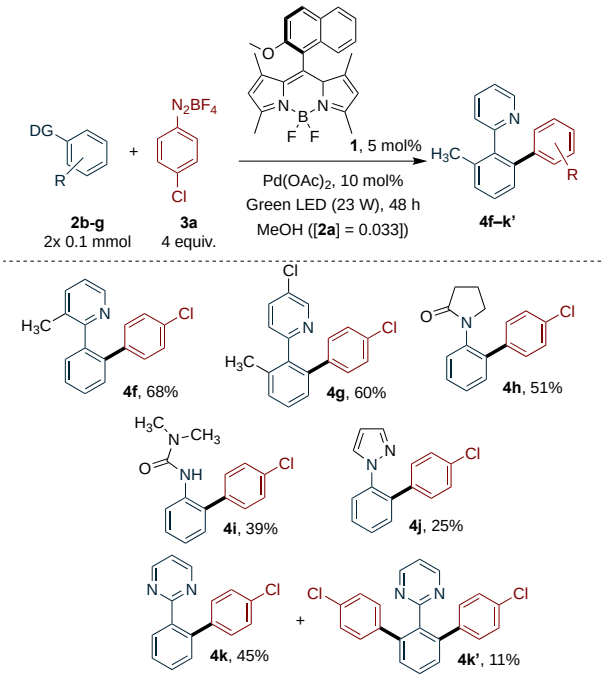

Scheme 2. Evaluation of different coordinating scaffolds.

With some differently substituted pyridines (**2b,c**) the reaction performed in the optimized conditions gave satisfactory yields of product. Other chelating groups, able to direct the palladium towards the C–H activation step were also compatible with the conditions. Amides, pyrazole, ureas, and pyrimidines were tested with the diazonium salt **3a**, and the reaction was giving from low to moderate yields. In the case of pyrimidine derivative (**3g**), we have observed the double insertion of aryl group. With the 4-fluorodiazonium salt **3e**, the reaction with substrates **2i** and **2e** gave, as observed in the previous reaction, by-product due to S_NAr substitution (Scheme 3).

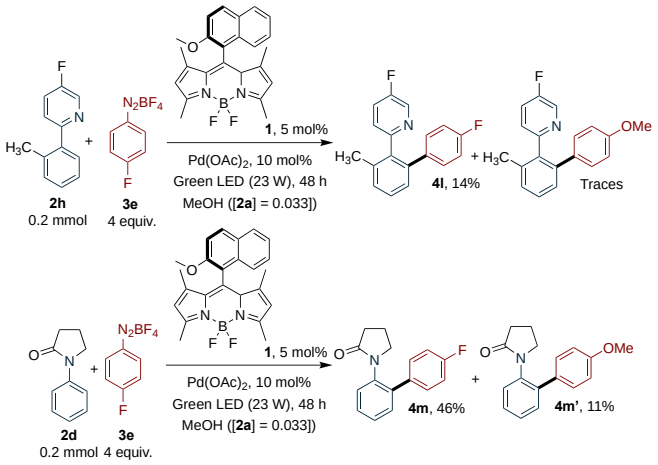

Scheme 3. Arylation of different coordinating substrates with diazonium salt **3e.**

In the case of the substrate **4h**, it is possible to compare our results with the one reported in literature using different organic dye.[31] The yields obtained with our BODIPY dye are inferior with respect to the use of acridine dye (52 vs 72% respectively), but the amount of $Pd(OAc)_2$ used in our reaction was lower (10 mol% vs 15 mol%). Unfortunately, pyridyl arene substrates were not further investigated with organic dyes and the other reported substrates are different, so that a direct comparison is not possible. With respect to the original contribution published by Sanford,[27] the yield obtained for **4b** by us are quite similar to the one obtained in the previous paper (72 vs 76% respectively) and the yields in the case of other substrates are comparable. Sandford obtained comparable results with the same amount of $Pd(OAc)_2$ (10 mol%) but in less time employing $[Ru(bpy)_3]Cl_2$ as photocatalyst.
The photophysical characterization of **BDP** was performed in the optimized reaction's solvent and does not significantly differ from the above-described results in MeCN (see SI). The mechanistic study was performed by monitoring the change in the emission intensity of singlet oxygen upon addition of each one of the other species present in the reaction. In fact, the presence of a quencher decreases the intensity of $^1O_2$ emission since it competes with energy transfer from **BDP**'s T_1 to ground state molecular oxygen.
The biggest change was observed in the presence of the diazonium salt, which can quench T_1 quantitatively. This is also able to partially quench **BDP**'s fluorescence (Figure **S8–10**), thanks to the very high concentration of this species in the reaction conditions. On the contrary, all other species present in the reaction did not significantly change $^1O_2$ emission intensity or the lifetime of **BDP**'s fluorescent excited state (Figure S8). This leads to hypothesize an oxidative quenching of the photosensitizer and the reaction mechanism depicted in Figure 5.

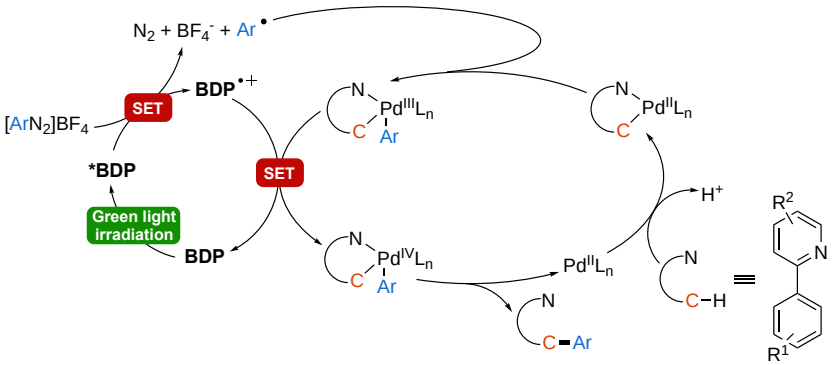

Figure 5. Hypothesized reaction mechanism.

It is finally important to highlight the photostability of the investigated BDP photosensitizer, as demonstrated in the present case by monitoring a diluted reaction mixture via UV-Vis spectroscopy Figure S11): this is a crucial aspect to be considered in a photoredox reaction.

Conclusion

In conclusion we have reported the first application in metallaphotoredox catalysis of a BODIPY dyad, that is able to populate its lowest-lying triplet excited state. The possibility of fine tuning the properties of BODIPY by varying the substituent of the aromatic ring positioned in *meso* positions make us confident in further developments in metallaphotoredox catalysis. We are exploring the BODIPY with other metals and reactions, expanding the use of these dyes with long living excited state.

Experimental Section

General procedure for dual photoredox and palladium-catalyzed room temperature C–H activation: all the reactions were performed in duplicate on 0.1 mmol scale of starting material **2a–h**. A dry 10 mL Schlenk tube, equipped with a Rotaflo stopcock, magnetic stirring bar and an argon supply tube, was first charged under argon with the organic photocatalyst **BDP** (**1**) (5 mol%, 0.005 mmol, 2 mg), $Pd(OAc)_2$ (10 mol%, 0.01 mmol, 2.3 mg) and the appropriate aryldiazonium salt (**3a-e**) (4 equiv., 0.4 mmol). Dry MeOH (3 mL to obtain a 0.033 M substrate solution) was then added, and the reaction mixture was further subjected to a freeze-pump-thaw procedure (four cycles) and the vessel refilled with argon. The reaction was irradiated under vigorous stirring for the desired time. After that the two reaction mixtures were quenched with a saturated solution of $NaHCO_3$ (7 mL approx.), combined and extracted with AcOEt (4 x 5 mL). The combined organic layers were dried over anhydrous Na_2SO_4 and the solvent was removed under reduced pressure. The crude was subject of flash column chromatography (SiO_2) to afford the products **4** in the stated yields.

Acknowledgements

Caterina Bellatreccia and Elena Del Giudice are gratefully acknowledged for their help with the photophysical measurements. National projects (PRIN 2017 20174SYJAF, SURSUMCAT and PRIN2017 20172M3K5N, CHIRALAB) are acknowledged for financial support of this research.

Keywords: BODIPY dyad • metallaphotoredox catalysis • Palladium • CH Activation • Arylheterocycles

[1] a) N. Holmberg-Douglas, D. A. Nicewicz, *Chem. Rev.* **2022**, *122*, 2, 1925-2016; b) F. Juliá, T. Constantin, D. Leonori, *Chem. Rev.* **2022**, *122*, 2292–2352; c) P. R. D. Murray, J. H. Cox, N. D. Chiappini, C. B. Roos, E. A. McLoughlin, B. G. Hejna, S. T. Nguyen, H. H. Ripberger, J. M. Ganley, E. Tsui, N. Y. Shin, B. Koronkiewicz, G. Qiu, R. R. Knowles, *Chem. Rev.* **2022**, *122*, 2, 2017–2291; d) L. Capaldo, D. Ravelli, M. Fagnoni, *Chem. Rev.* **2022**, *122*, 1875-1924; e) V. M. Lechner, M. Nappi, P. J. Deneny, S. Folliet, J. C. K. Chu, M. J. Gaunt, *Chem. Rev.* **2022**, *122*, 1752-1829; f) M. J. Genzink, J. B. Kidd, W. B. Swords, T. P. Yoon*, Chem. Rev.* **2022**, *122*, 1654-1716.

[2] a) V. Balzani, G. Bergamini, P. Ceroni, *Angew. Chem. Int Ed.* **2015**, *54*, 11320-11337; *Angew. Chem.* **2015**, *127*, 11474-11492; b) N. E S Tay, D. Lehnherr, T. Rovis, *Chem. Rev.* **2022**,122, 2487-2649.

[3] a) A. Y. Chan, I. B. Perry, N. B. Bissonnette, B. F. Buksh, G. A. Edwards, L. I. Frye, O. L. Garry, M. N. Lavagnino, B. X. Li, Y. Liang, E. Mao, A. Millet, J. V. Oakley, N. L. Reed, H. A. Sakai, C. P. Seath, D. W. C. MacMillan, *Chem. Rev.* **2022**, *122*, 1485–1542; b) K. P. S. Cheung, S. Sarkar, V. Gevorgyan, *Chem. Rev.* **2022**, *122*, 1543-1625.

[4] M. H. Shaw, J. Twilton, D. W. C. MacMillan, *J. Org. Chem.* **2016**, *81*, 6898–6926.

[5] L. Buzzetti, G. E. M. Crisenza, P. Melchiorre, *Angew. Chem. Int. Ed.* **2019**, *58*, 3730-3747; *Angew. Chem.* **2019**, *131*, 3768-3786.

[6] N. A. Romero, D. A. Nicewicz, *Chem. Rev.* **2016**, *116*, 17, 10075–10166.

[7] A. Gualandi, M. Anselmi, F. Calogero, S. Potenti, E. Bassan, P. Ceroni P. G. Cozzi, *Org. Biom. Chem.* **2021**, *19*, 3527-3550.

[8] E. Bassan, A. Gualandi, P. G. Cozzi, P. Ceroni, *Chem. Sci.* **2021**, *12*, 6607-6628.

[9] J. Zhao, K. Xu, W. Yang, Z. Wanga, F. Zhong, *Chem. Soc. Rev.* **2015**, *44*, 8904-8939.

[10] T. Yogo, Y. Urano, Y. Ishitsuka, F. Maniwa, T. Nagano, *J. Am. Chem. Soc.* **2005**, *127*, 12162–12163.

[11] A. Kamkaew, S. H. Lim, H. B. Lee, L. V. Kiew, L. Y. Chung, K. Burgess, *Chem. Soc. Rev.* **2013**, *42*, 77 – 88.

[12] P. De Bonfils, L. Péault, P. Nun, V., Coeffard, *Eur. J. Org. Chem.* 2021, 1809-1824.

[13] A. M. Durantini, L. E. Greene, R. Lincoln, S. R. Martínez, G. Cosa, *J. Am. Chem. Soc.* **2016**, *138*, 1215–1225.

[14] M. A. Filatov, *Org. Biomol. Chem.* **2020**, *18*, 10-27.

[15] For further details on the mechanism, please refer to ref. [8].

[16] W. Li, L. Li, H. Xiao, R. Qi, Y. Huang, Z. Xie, X. Jing, H. Zhang, *RSC Adv.* **2013**, *3*, 13417–13421.

[17] G. Bolat, F. Kuralay, B. Temelli, C. Unaleroglu, S. Abaci, *Polym. Bull.* **2015**, *72*, 867–879.

[18] a) G. Magagnano, A. Gualandi, M. Marchini, L. Mengozzi, P. Ceroni, P. G. Cozzi, *Chem. Commun*. **2017**, *53*, 1591-1594; b) A. Da Lama, B. Bartolomei, C. Rosso, G. Filippini, M. M. Martínez, L. A. Sarandeses, M. Prato., *Eur. J. Org. Chem.* **2022**, e202200622.

[19] P. Ranaa, N. Singh, P. Majumdar, S. Prakash Singh, *Coord. Chem. Rev.* **2022**, *470*, 214698.

[20] L. Yang, Z. Huang, G. Li, W. Zhang, R. Cao, C. Wang, J. Xiao, D. Xue, *Angew. Chem. Int. Ed.* **2018**, *57*, 1968-1972; *Angew. Chem.* **2018**, *130,* 1986-1990.

[21] A. Juris, V. Balzani, P. Belser, A. von Zelewsky, *Helv. Chim. Acta* **1981**, *64*, 2175–2182.

[22] a) A. C. Benniston, G. Copley, K. J. Elliott, R. W. Harrington, W. Clegg, *Eur. J. Org. Chem.* **2008**, 2705-2713; b) M. Brçring, R. Krüger, S. Link, C. Kleeberg, S. Kçhler, X. Xie, B. Ventura, L- Flamigni. *Chem. Eur. J.* **2008**, *14*, 2976 – 2983.

[23] V. Balzani, P. Ceroni. A. Juris in "*Photochemistry and Photophysics: Concepts, Research, Applications", Wiley, 2014.*

[24] A. B. Nepomnyashchii, A. J. Bard, *Acc. Chem. Res.* **2012**, *45*, 1844–1853. For comparison of the potentials naphthyl-BODIPY dye with other known BODIPY dyes, see: a) B. L. Thompson, Z. Heiden. In: BODIPY Dyes - A Privilege Molecular Scaffold with Tunable Properties. J. Bañuelos-Prieto, R. S. Llano (Eds.), IntechOpen. **2018**, https://doi.org/10.5772/intechopen.79704.

[25] V. G. Plotnikov, *Int. J. Quantum Chem.* **1979**, *16*, 527–541.

[26] a) Y.-L. Chen, S.-W. Li, Y. Chi, Y.-M. Cheng, S.-C. Pu, Y.-S. Yeh, P.-T. Chou, *ChemPhysChem* **2005**, *6*, 2012–2017; b) J. Zhang, S. Mukamel, J. Jiang, *J. Phys. Chem. B* **2020**, *124*, 2238–2244; c) Y. Dong, P. Kumar, P. Maity, I. Kurganskii, S. Li, A. Elmali, J. Zhao, D. Escudero, H. Wu, A. Karatay, O. F. Mohammed, M. Fedin, *Phys. Chem. Chem. Phys*. **2021**, *23*, 8641–8652.

[27] D. Kalyani, K. B. McMurtrey, S. R. Neufeldt, M. S. Sanford, *J. Am. Chem. Soc.* **2011**, *133*, 18566–18569.

[28] For the use of Pd complexes in photoredox catalysis, see: a) P. Chuentragool, D. Kurandina, V. Gevorgyan, *Angew. Chem. Int. Ed.* **2019**, *58*, 11586-11598; *Angew. Chem.* **2019,** *131*, 11710-11722; b) M. Sheea, N. D. Pradeep Singh, *Catal. Sci. Technol.*, **2021**,*11*, 742-767; c) P. Sarathi Saha, P. Gopinath, *Eur. J. Org. Chem.* **2022**, e202200733.

[29] a) D. P. Hari, B. König, *Angew. Chem. Int. Ed.* **2013**, *52*, 4734-4743; *Angew. Chem.* **2013**, *125*, 4832-4842; b) S. Sarath Babu, P. Muthuraja, P. Yadav, P. Gopinath, *Adv. Synth. Catal.* **2021**, *363*, 1782-1809; c) X. Zhang, Y. Mei, Y. Li, J. Hu, D. Huang, Y. Bi, *Asian. J. Org. Chem.* **2021**, *10*, 453-463.

[30] a) J. Zhang, J. Chen, X. Zhang, X. Lei, *J. Org. Chem.* **2014**, *79*, 10682–10688; b) L. Liang, M.-S. Xie, H.-X. Wang, H-Y. Niu, G.-R. Qu, H.-M. Guo, *J. Org. Chem.* **2017**, *82*, 5966–5973; c) S. Sarath Babu, M. Shahida, P, Gopinath, *Chem. Commun.*, **2020**,56, 5985-5988.

[31] J. Jiang, W.-M. Zhang, J.-J. Dai, J. Xu, H.-J. Xu, *J. Org. Chem.* **2017**, *82*, 3622–3630.
[32] M. K. Sahoo, S. P. Midya, V. G. Landge, E. Balaraman, *Green Chem.* **2017**,*19*, 2111-2117.